Radboud Repository

Radboud University Nijmegen

PDF hosted at the Radboud Repository of the Radboud University Nijmegen

The following full text is a publisher's version.

For additional information about this publication click this link.
http://hdl.handle.net/2066/115612

THREE-DIMENSIONAL CHARACTER OF SEMIMETALLIC InAs–GaSb SUPERLATTICES

J.C. Maan

Max-Planck Institut für Festkörperforschung, Hochfeld-Magnetlabor, 38042 Grenoble, France

Y. Guldner, J.P. Vieren, P. Voisin and M. Voos

Groupe de Physique des Solides de l'Ecole Normale Supérieure,* Tour 23, 2 place Jussieu, 75005 Paris, France

and

L.L. Chang and L. Esaki

IBM Thomas J. Watson Research Center, P.O. Box 218, Yorktown Heights, NY 10598, U.S.A.

High-field, far-infrared magneto-absorption experiments are performed in semimetallic InAs–GaSb superlattices. The spectra exhibit extensive oscillations of cyclotron resonance and interband absorptions from valence to conduction subbands. Transitions at both the center and the boundary of the superlattice zone are observed, from which the width of the ground conduction subband is obtained, demonstrating directly its three-dimensional character.

A CHARACTERISTIC FEATURE of the InAs–GaSb superlattice is the occurrence [1] of a semiconductor–semimetal transition when the InAs layer thickness becomes ∼ 100 Å. This transition arises from the peculiar band alignment of the basic materials; the bottom of the InAs conduction band being 150 meV below the top of the GaSb valence band. Another inherent feature of this superlattice is associated with the extremely light electron mass of InAs. Its de Broglie wavelength is so long that, even for GaSb layer thickness in excess of 100 Å, there is considerable interaction between electrons in successive InAs layers which leads to conduction subbands with a substantial width in the range of tens of millivolts. This subband width manifests the quasi-three-dimensional character of a superlattice, as opposed to the situation arising from a simple quantum size effect.

The band structure of such a semimetallic superlattice is schematically shown in Fig. 1(a) along k_z, where z is the direction perpendicular to the layers. The ground conduction subband E_1 is below the ground valence subband H_1. The conduction states are mainly localized in the InAs layers, and the valence states in the GaSb layers [1, 2]. The width of E_1 is here ΔE_1 but that of H_1 is essentially zero [2, 3]. In the semimetallic samples, electrons transfer from H_1 to E_1, namely from GaSb to InAs, and the Fermi level E_F is close to H_1.

Under magnetic fields, both E_1 and H_1 exhibit a series of Landau levels, which move upward and downward, respectively, with an increase in the field. Clearly, each Landau level of H_1 gives rise to a single peak in the density of states. The E_1 subband, on the other hand, being flat at the superlattice zone center, $k_z = 0$, and the zone boundary, $k_z = \pm \pi/d$, where d is the superlattice periodicity, results in a doublet or two peaks in the density of states for each Landau level as shown in Fig. 1(b). If the selection rules for interband transitions are taken to be [4] $\Delta k_z = 0$ and $\Delta N = 0$, where N is the Landau level index, two sets of transitions are thus possible at these two extremal points. Note that such interband transitions can occur because the electron and hole wavefunctions overlap.

We wish to present in this communication far-infrared magneto-absorption experiments in semimetallic InAs–GaSb superlattices, similar to those reported earlier in establishing the negative energy gaps [4]. With the use of a high magnetic field and an optically pumped laser to provide a large number of infrared wavelengths, we have observed extensive transitions associated with both cyclotron resonance and interband absorptions with Landau indices covering the range of $N = 1$ to 7. These results not only substantiated the semimetallic property of the superlattice but provided accurate determinations of the subband energies of E_1 and H_1 at $k_z = 0$. What is more significant is the observation of the transition between Landau levels at $k_z = \pm \pi/d$. The width of the E_1 subband has for the first time been

---

Table 1. Thickness of the InAs (d_1) *and* GaSb (d_2) *layers for samples* S1 *and* S2. *Also given are the experimental and theoretical values of* E_1, H_1 *and* ΔE_1

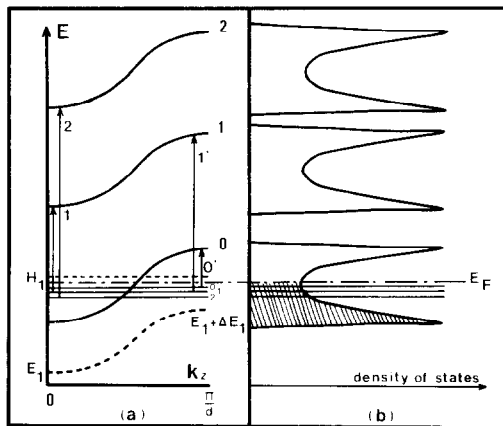| Samples	d_1 (Å)	d_2 (Å)	Theory (LCAO) (meV)			Experiment (meV)		
			E_1	ΔE_1	H_1	E_1	ΔE_1	H_1
S1	120	80	87.5	21	129.5	100 ± 15	23 ± 1	139 ± 15
S2	200	100	64.5	16	132.5	70 ± 10	19 ± 1	128 ± 10

Fig. 1. (a) Schematic band structure of a semimetallic InAs–GaSb superlattice along k_z. The dashed curves are without magnetic field, the solid curves are the corresponding Landau levels under magnetic field, and E_F is the Fermi level. Transitions noted 1, 2 correspond to transitions at $k_z = 0$ from H_1 Landau levels up to E_1 Landau levels with the same index, namely $N = 1, 2$. Those noted $0'$, $1'$ correspond to similar transitions at $k_z = \pi/d$, with $N = 0, 1$. (b) Density of states associated with the E_1 and H_1 subbands under magnetic field. The hatched area corresponds to states occupied by electrons.

measured experimentally, which indicates directly that the electron system in a superlattice possesses a three-dimensional character, deviating from strict two-dimensionality.

The samples (S1 and S2) used here were grown [1] by molecular-beam epitaxy on (100) GaSb substrates, the total thickness of the superlattice being typically $\sim 2\,\mu$m. The thicknesses of the InAs and GaSb layers are given in Table 1 for both samples. Experimentally, the FIR transmission of these superlattices is studied at fixed photon energies as a function of the magnetic field B. The infrared radiation is propagating parallel to B (Faraday configuration), which is applied perpendicular to the plane of the layers. The field was provided by a Bitter magnet and could be varied continuously from 0 to 20 T. Several FIR wavelengths were generated using an optically pumped FIR laser with CH_3OH as the active medium ($\lambda = 1217, 699, 570, 471, 394, 294, 254, 233, 203, 193, 170, 118, 96$ and $70\,\mu$m). The transmission
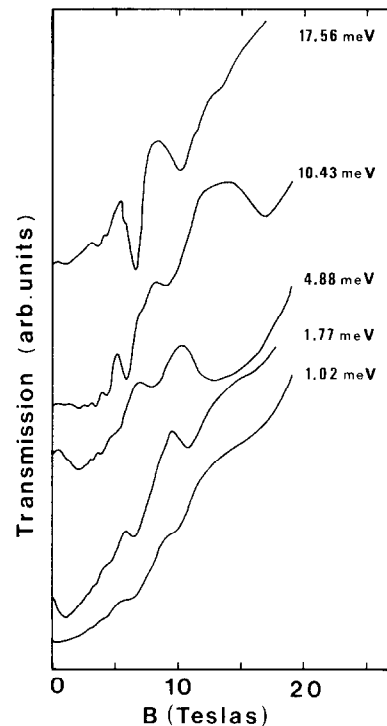

Fig. 2. Transmission signals vs. magnetic field observed at liquid helium temperature in sample S1 for different infrared photon energies.

signal was measured with a Ge bolometer cooled at liquid helium temperature, and normalized to the incident radiation intensity with a reference signal detected with a Golay cell to eliminate fluctuations of laser instabilities.

Typical transmission spectra obtained at liquid helium temperature are presented in Fig. 2 for sample S1, where it can be seen that, for each infrared wavelength, the transmission signal as a function of B exhibits several minima. In Fig. 3 are presented the infrared energy positions of the transmission minima (or absorption maxima) vs. B. As shown below from theoretical analyses, the energies corresponding to the transmission minima depend almost linearly on B. Extrapolation to zero field results in $h\nu = 0$ for the line marked CR in Fig. 3(a), an energy of ~ 39 meV for the family of lines
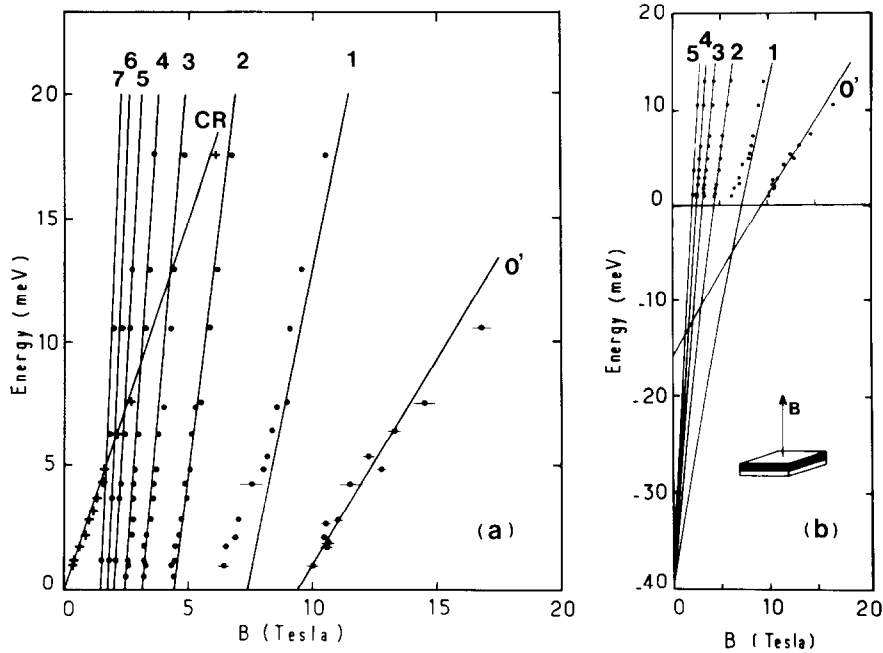
Fig. 3. Position of the transmission minima (see Fig. 2) as a function of the infrared photon energy and magnetic field B (crosses and full dots). The solid lines correspond to theoretical fits using the model presented in the text. The inset shows schematically the geometry of the experiment.

designated $1, 2, 3, \ldots$ in Figs. 3(a) and 3(b), and an energy of -16 meV for the single line which is denoted as $0'$ in the same figures. The CR line is interpreted as being due to electron cyclotron resonance, i.e. to transitions from the last filled to the first empty Landau level of E_1. The curves which converge to the most negative energy are attributed to interband transitions from H_1 to E_1 Landau levels at $k_z = 0$, such as those noted 1 and 2 in Fig. 1(a). The $0'$ line is also attributed to similar interband transitions, but it occurs at $k_z = \pi/d$ as illustrated in Fig. 1(a). These interpretations in terms of both cyclotron resonance and interband transitions are consistent with those reported earlier [4]. The observations of additional transitions associated with the 1 and $0'$ branches are made possible by the application of high fields in the present experiments.

Quantitatively the E_1 and H_1 Landau levels are calculated as were done previously [4, 5], taking into account the InAs conduction band non-parabolicity on the basis of the two-band $k \cdot p$ model due to Kane [6]. For the E_1 subband one obtains for the Nth Landau level:

$$E_{1,N} = -\frac{E_G}{2} + \left[\left(\frac{E_G}{2}\right)^2 + E_G D_N\right]^{1/2} \quad (1)$$

with $D_N = (N + 1/2)\hbar\omega_c + E_1(1 + E_1/E_G)$ and $\omega_c = eB/m_e^*$ where E_G and m_e^* are respectively the band gap and band edge mass of bulk InAs. For the $H_{1,N}$ Landau level, we take simply $H_{1,N} = H_1 - (N + 1/2)\hbar\omega_v$,

with $\omega_v = eB/m_h^*$ where m_h^* is the GaSb heavy hole effective mass. All the energies used here are measured from the bulk InAs conduction band edge.

For electron cyclotron resonance transitions, $h\nu = E_{1,N+1} - E_{1,N}$, where N is such that $E_{1,N}$ is below, and $E_{1,N+1}$ above, the Fermi level E_F. Interband transitions occurring at $k_z = 0$ from H_1 Landau levels up to E_1 Landau levels correspond to $h\nu = E_{1,N} - H_{1,N}$, taking also here $E_F = H_1$ and the same selection rules as in [4]. Fits of our experimental data to this theoretical model are shown in Fig. 3 for sample S1, with $m_e^* = 0.023\, m_0, E_G = 410$ meV and $m_h^* = 0.33\, m_0$ [7]. The agreement between experiment and theory is quite good and, from these fits, we obtain the values of E_1 and H_1 at $B = 0$ which are listed [8] in Table 1. Similar studies were done in sample S2, and the corresponding values of these parameters are also given in Table 1. We can, in addition, determine the superlattice electron cyclotron mass m^* from the CR data, which is found to be [8] $0.0385 m_0$ and $0.0375 m_0$ in samples S1 and S2, respectively, with an uncertainty of $\pm 0.0015 m_0$.

Having established the values of E_1 and H_1, we can calculate the transition energies at $k_z = \pi/d$ from the same theoretical model, replacing E_1 by $E_1 + \Delta E_1$ in equation (1). Figure 3 shows the results fitted to the data points from which the Landau index is identified, $N = 0'$, and the bandwidth is obtained, $\Delta E_1 = 23$ meV. This value together with that obtained from sample S2 is also listed in Table 1. To observe the transition at $k_z = \pi/d$ requires that the subband broadening from

scattering be smaller than the subband width itself. This is borne out from the scattering time of $\sim 5 \times 10^{-13}$ sec as estimated from the cyclotron resonance linewidth, which corresponds to a level broadening of ~ 1.2 meV. That transitions associated with higher Landau indices at this zone boundary are not observed experimentally can be understood from considerations of wavefunction overlap between electrons and holes [9]. For a given energy, the E_z component at $k_z = \pi/d$ is higher than that at $k_z = 0$ by the amount of ΔE_1. This brings the former closer to the valence band edge of GaSb as such its associated electron wavefunction is more localized in InAs. For a given magnetic field, transitions at π/d are expected to be weaker than at 0, so that they can be resolved only in regions where transitions at $k_z = 0$ are not present. It is clear from Table 1, where calculated values of E_1, H_1 and ΔE_1 by the LCAO method are also included, that the experimental and theoretical results compare quite favorably in all cases.

The systematic deviation around 8 T of the data points from the calculated curve for the $N = 1$ transition, as can be seen in Fig. 3, is not understood at present. This may be due to polaron effects, which have been observed for interband transitions [10]. The effects become important at magnetic field values when the energy separation between the $N = 0$ and the $N = 1$ Landau levels, for example, approaches the longitudinal optical phonon energy. That the LO-phonon energy of InAs (and GaSb) is [7] about 30 meV is consistent with our data. Recent calculations [11] have shown that the magneto-optical anomalies arising from electron–phonon interactions are considerably enhanced in superlattices.

To conclude, we have observed in semimetallic InAs–GaSb superlattices cyclotron resonance and interband transitions at $k_z = 0$, from Landau levels of the ground valence subband H_1 up to those of the ground conduction subband E_1. We have obtained extensive experimental data, corroborating earlier results reported previously [4]. In addition, we have determined the width ΔE_1 of the ground conduction subband, demonstrating directly the quasi-three-dimensional character of these superlattices. Finally, we have obtained from these investigations values of E_1, H_1 and ΔE_1 which compare favorably with those calculated by the LCAO method [2].

REFERENCES

1. For a recent review see, for example, L.L. Chang & L. Esaki, *Surf. Sci.* **98**, 70 (1980).
2. G.A. Sai-Halasz, L. Esaki & W.A. Harrison, *Phys. Rev.* **B18**, 2812 (1978).
3. Note that H_1 corresponds to heavy holes (see, for example, [1]).
4. Y. Guldner, J.P. Vieren, P. Voisin, M. Voos, L.L. Chang & L. Esaki, *Phys. Rev. Lett.* **45**, 1719 (1980).
5. H. Bluyssen, J.C. Maan, P. Wyder, L.L. Chang & L. Esaki, *Solid State Commun.* **31**, 75 (1979).
6. E.O. Kane, *J. Phys. Chem. Solids* **1**, 249 (1957).
7. The InAs and GaSb parameters can be found in *Handbook of Electronic Materials* (Edited by M. Neuberger), Vol. 2. Plenum, New York (1971).
8. The values of E_1, H_1 and m^* obtained here are somewhat different from those reported in [4]. This is due to different values of the InAs band gap used in the theoretical fits. Indeed, the fits shown in [4] were done with a gap of 420 meV, not 410 meV as erroneously written in the text.
9. G.A. Sai-Halasz, L.L. Chang, J.M. Welter, C.A. Chang & L. Esaki, *Solid State Commun.* **26**, 935 (1978).
10. E.J. Johnson & D.M. Larsen, *Phys. Rev. Lett.* **16**, 655 (1966).
11. S. Das Sarma & A. Madhukar, *Phys. Rev.* **B22**, 2823 (1980).